

Rewiring of hindlimb corticospinal neurons after spinal cord injury

Arko Ghosh^{1,4}, Florent Haiss², Esther Sydekum³, Regula Schneider¹, Miriam Gullo¹, Matthias T Wyss², Thomas Mueggler³, Christof Baltes³, Markus Rudin^{2,3}, Bruno Weber² & Martin E Schwab¹

Little is known about the functional role of axotomized cortical neurons that survive spinal cord injury. Large thoracic spinal cord injuries in adult rats result in impairments of hindlimb function. Using retrograde tracers, we found that axotomized corticospinal axons from the hindlimb sensorimotor cortex sprouted in the cervical spinal cord. Mapping of these neurons revealed the emergence of a new forelimb corticospinal projection from the rostral part of the former hindlimb cortex. Voltage-sensitive dye (VSD) imaging and blood-oxygen-level-dependent functional magnetic resonance imaging (BOLD fMRI) revealed a stable expansion of the forelimb sensory map, covering in particular the former hindlimb cortex containing the rewired neurons. Therefore, axotomised hindlimb corticospinal neurons can be incorporated into the sensorimotor circuits of the unaffected forelimb.

Large spinal cord injuries result in the disruption of descending and ascending sensorimotor circuits, but most corticospinal neurons survive the injury^{1–3}. In intact animals, the neurons of the corticospinal tract (CST) are essential for the initiation and control of skilled movements. Although it has been shown that these neurons survive after injury, their functional role remains unknown. Spinal cord injuries can induce sprouting of descending motor pathways at several levels of the adult CNS^{4,5}, and corticospinal neurons have been shown to sprout in the spinal cord of adult rodents and primates^{6–10}. What functions do these neurons exert and what inputs do these re-wired cortical neurons receive?

Electrophysiological studies have shown that the somatosensory cortex can be physiologically remodeled after spinal cord injuries in primates^{11,12}. Denervated cortical areas can be reactivated by expanding representations of unaffected body parts, probably accompanied by remodeling of subcortical and cortical connectivity. In adult rats, it is unclear whether sensory representations reorganize after spinal cord injury and to what extent anatomical rewiring occurs. A thoracic bilateral dorsal spinal cord hemisection in the adult rat results in hindlimb paresis. In this injury, the hindlimb cortex is deprived of tactile and proprioceptive inputs, and corticospinal axons originating from this cortex are axotomized. Interestingly, after the thoracic injury in rodents, some corticospinal axons originating from the hindlimb cortex were seen to sprout into the cervical spinal cord, far rostral of the injury site^{7,8}. This anatomical rearrangement was accompanied by the occurrence of forelimb movements upon electrical microstimulation of the hindlimb cortex⁸. However, the functionality of these neurons remained unknown. If the sprouting corticospinal neurons are to be incorporated into the forelimb circuitry, forelimb

sensory input must reach these neurons and intracortical connectivity must be modified in line with the changes in the CST. Whether the denervated hindlimb cortex can be activated by sensory input from the forelimbs remains unresolved in the light of apparently contradictory findings from previous studies^{13–15}.

We created large thoracic lesions in adult rats that resulted in increased behavioral dependence of the animals on the forelimb in the absence of functional hindlimbs. Using retrograde tracings from the spinal cord we identified and mapped axotomised corticospinal neurons in the hindlimb cortex that were rewired to the cervical spinal cord. Many sprouting fibers originated from the hindlimb field. Subsets of these neurons remained rewired to the cervical spinal cord several months later. VSD imaging and BOLD fMRI of the sensorimotor cortex revealed that the forelimb representation was expanded after injury. The enlarged forelimb representation included those parts of the hindlimb sensorimotor cortex that gave rise to the rewired corticospinal neurons. By recording action potentials from axotomized hindlimb corticospinal neurons, we found that they responded faster to forelimb sensory input than when intact. Together, these results show that axotomised corticospinal neurons rewire rostral to the injury to become forelimb neurons. These neurons might be functionally relevant to the motor control of the unaffected body parts.

RESULTS

Forelimb use after thoracic spinal cord injury

Large thoracic bilateral dorsal hemisections of the rat spinal cord (Fig. 1a and Supplementary Fig. 1) resulted in severe hindlimb paresis with little spontaneous recovery^{16,17}. We assessed limb movements during overground locomotion on a runway (Catwalk^R) that measured

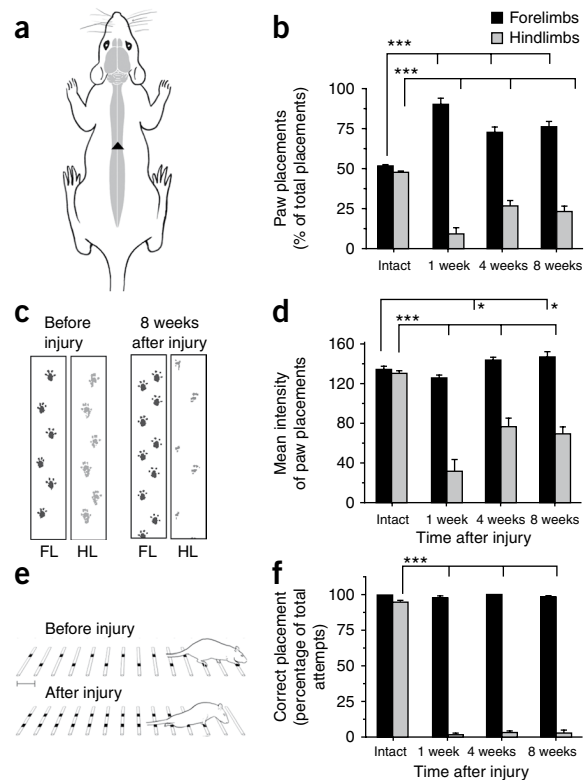
¹Brain Research Institute, University of Zurich and Swiss Federal Institute of Technology Zurich, Zurich, Switzerland. ²Institute of Pharmacology and Toxicology, University of Zurich, Zurich, Switzerland. ³Institute for Biomedical Engineering, University of Zurich and Swiss Federal Institute of Technology Zurich, Zurich, Switzerland. ⁴Present address: Institute of Neuroinformatics, University of Zurich and Swiss Federal Institute of Technology Zurich, Zurich, Switzerland. Correspondence should be addressed to A.G. (arko@ini.phys.ethz.ch).

Received 21 July; accepted 15 October; published online 13 December 2009; doi:10.1038/nn.2448

Figure 1 Behavioral analysis after a thoracic spinal cord injury. (a) The injury at the T8 segment of the spinal cord (black arrowhead) resulted in paralyzed hindlimbs. (b) Quantification of the number of fore- and hindlimb steps taken while crossing the horizontal runway. (c) Paw prints made by a rat before and eight weeks after injury, captured using the analysis system (Catwalk). (d) Mean pixel intensities (arbitrary unit) of paw placements measured using the analysis system. (e) Schematic representation of animals crossing a horizontal ladder used to evaluate their skilled movements before and after injury. Black marks on the rung denote forelimb placements. Scale bar, 6 cm. (f) Quantification of the number of correct placements on the horizontal ladder. $n = 13$ rats, error bars represent \pm s.e.m., data was subjected to t -test (unpaired, two-tailed), * $P < 0.05$, *** $P < 0.001$.

the number of paw placements and the intensity of the foot prints (indicating the amount of bodyweight supported)¹⁸. Intact animals walked on the runway with alternating fore- and hindlimb steps (Fig. 1b,c). The thoracic injury (at vertebra T8) resulted in a marked reduction of hindlimb use and the forelimbs were used extensively to cross the runway. The forelimbs propelled the body forward, dragging the paralyzed hindlimbs. The forelimbs performed $90 \pm 3.4\%$ (\pm denotes s.e.m.) of the steps after injury compared to $52 \pm 0.34\%$ in intact animals ($P = 9.18 \times 10^{-10}$, Fig. 1b,c). At both four and eight weeks after injury, forelimb use remained high even though the hindlimb recovered some stepping ability. This spontaneous recovery of the hindlimb was very poor; the hindlimbs were not used as much as before injury and even when they were used to step, the body weight supported was much lower (Fig. 1b,d). The forelimbs also showed greater weight bearing after injury (135 ± 2.87 pixel intensity (arbitrary unit)¹⁸) in intact rats compared with 145 ± 2.55 4 weeks after injury, $P = 0.015$).

We evaluated the animals as they crossed a horizontal ladder as a test of precise sensory-guided paw placements (Fig. 1e,f). This task depends strongly on sensory input and descending motor control, including that carried by the CST¹⁹. Trained intact animals crossed the ladder with ease, making regular forelimb and hindlimb steps ($100 \pm 0.0\%$ correct forelimb placements and $95 \pm 1.5\%$ correct hindlimb placements). After spinal cord injury, the animals crossed the ladder with great difficulty. The hindlimbs were often dragged along; the forelimbs gripped the rungs and enabled the rats to cross the ladder.



The drop in the success rate of the hindlimb on the horizontal ladder after injury ($2 \pm 0.8\%$ correct placements 1 week after injury) persisted till the last time point of assessment at 8 weeks ($3 \pm 2.0\%$ correct placements at 8 weeks after injury). Therefore, in the skilled task of crossing the horizontal ladder, paraparetic rats were entirely dependent on their forelimbs in the absence of functional recovery of the hindlimbs.

Reorganization of axotomized hindlimb corticospinal axons

In acutely injured animals, careful retrograde labeling of the corticospinal neurons that project to the cervical gray matter with the dye

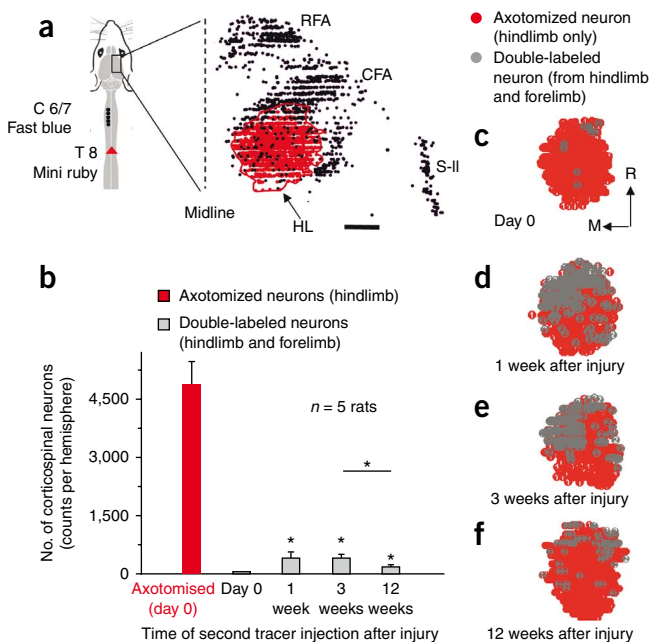
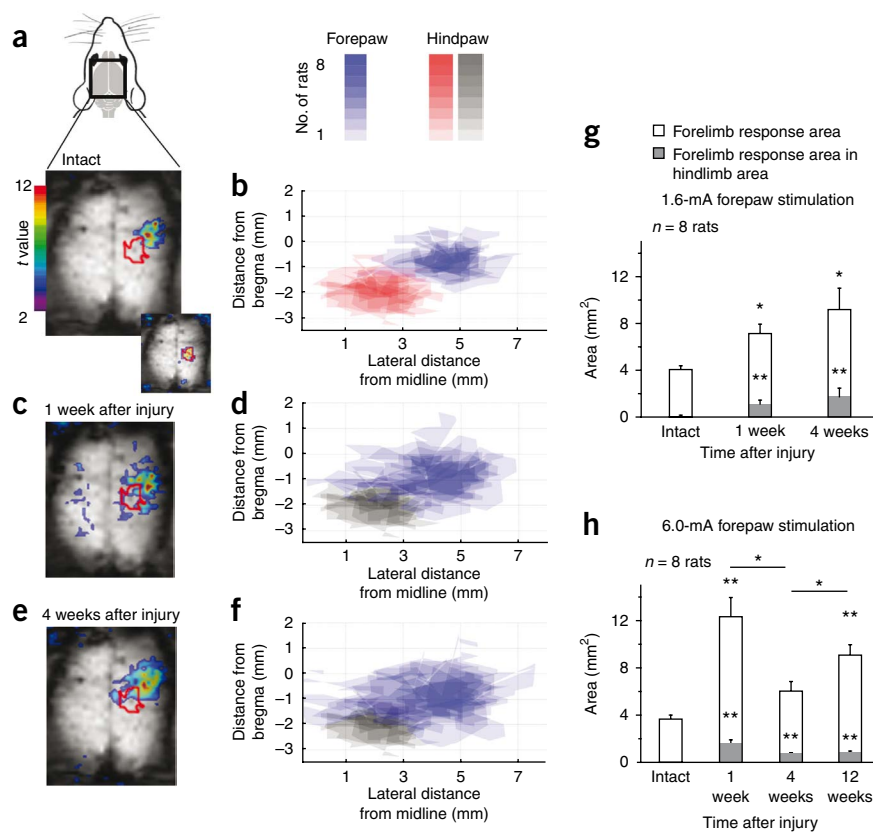


Figure 2 Retrograde labeling of hindlimb corticospinal neurons projecting to the cervical spinal cord gray matter. (a) A representative non-flattened cortical map of retrograde-labeled neurons in an acutely injured animal (horizontal plane of view of the reconstruction); red dots indicate hindlimb corticospinal neurons, black dots indicate neurons projecting to the cervical spinal cord (forelimb corticospinal neurons). The retrograde tracer Mini Ruby was placed at the site of injury (red arrowhead, T8) and a second tracer, Fast Blue, was injected unilaterally into the cervical spinal cord gray matter at five injection sites (C6/7, black spots). RFA: rostral forelimb area, CFA: caudal forelimb area, S-II: secondary somatosensory area, HL: hindlimb corticospinal representation. Scale bar, 1 mm. (b) Quantification of double-labeled neurons in the cortical hemisphere contralateral to injection in intact and injured rats. Y axis denotes cell counts from the hemisphere contralateral to the injection as shown in a (derived from 50- μ m-thick brain sections collected with a 100- μ m gap). In acutely injured rats, a very small proportion of the axotomized hindlimb neurons (red bar) were double-labeled (also projecting to the forelimb (gray bars)). (c-f) Representative maps of double-labeled (axotomized hindlimb corticospinal neurons projecting to the cervical spinal cord) and single-labeled (axotomized corticospinal neurons without detectable uptake from the cervical cord) in the sensorimotor cortex at different time points after injury. R, rostral. M, medial. $n = 5$ rats, error bars represent \pm s.e.m., data was subjected to Mann-Whitney U test, * $P < 0.05$.

Figure 3 BOLD-fMRI mapping of forelimb activation in the sensory motor cortex before and after injury. (**a,c,e**) Representative gradient-echo EPI scans (horizontal plane of view) with BOLD-fMRI activation map in a rat before injury (**a**), 1 week after injury (**c**) and 4 weeks after injury (**e**) in response to forepaw stimulation (1.6 mA). Insert in **a** shows the location of the hindlimb in the same animal before injury. In **a, c** and **e** the red line depicts the hindlimb area. (**b,d,f**) Superimposed activation maps of intact rats (**b**) and rats 1 (**d**) or 4 (**f**) weeks after injury. Blue and red areas show the activation after forepaw and hindpaw stimulation, respectively. After injury, there is no response from the hindpaw; the original area is repeated in gray (**d,f**). (**g,h**) Mean forelimb representation area (black outlined columns) and forelimb-hindlimb overlap area (gray columns) in response to 1.6 mA (**g**) and 6 mA (**h**) forelimb stimulation. Statistics on area quantifications are as described in **Figure 2**. Maps were derived without flattening the cortical surface.



Fast Blue (without labeling the neighboring, densely packed, CST), followed by application of another tracer (Mini Ruby) to the cut CST axons revealed the separation of the forelimb and hindlimb corticospinal representations in the sensorimotor cortex (**Fig. 2a**). Although hindlimb corticospinal neurons appeared from a confined area of the sensorimotor cortex, forelimb neurons appeared from a much larger area. Forelimb CST fibers primarily originate from the caudal forelimb area (CFA, homologous to primary motor cortex in primates²⁰) and from the rostral forelimb area (RFA, homologous to premotor motor cortex and supplementary motor area in primates²¹). In agreement with previous studies, we found that only a few of these forelimb neurons in the hindlimb field were double-labeled with the two retrograde tracers (27.6 ± 2.2 , counts per hemisphere contralateral to the cervical injection); that is, they were neurons with fibers that projected both to the cervical spinal cord and to the lower thoracic or lumbo-sacral cord (**Fig. 2b,c**)²².

When the tracer Fast Blue was injected in the cervical gray matter 1 week, 3 weeks or 12 weeks after spinal cord injury (Mini Ruby placed at the injury site), there was a significant increase in the number of double-labeled cells (**Fig. 2b**). One week after injury, the number of double-labeled cells increased to 393 ± 144 ($P = 0.01$). Axotomized fibers originating mainly from the rostral regions of the hindlimb sensorimotor cortex projected more frequently to the cervical spinal cord, forming a dense cluster of double-labeled cells (**Fig. 2d**). Three weeks after injury, the number of double-labeled cells remained high (**Fig. 2b,e**), but at twelve weeks there was a significant decrease in the number of double-labeled cells (158 ± 28 compared to 384 ± 90 at 3 weeks, $P = 0.04$). These cells were preferentially located in the rostral hindlimb field (**Fig. 2f**). Over the course of 12 weeks, the total number of retrogradely labeled axotomized hindlimb corticospinal neurons did not alter significantly ($4,866 \pm 602$ in acutely injured animals, $3,319 \pm 27$ twelve weeks after injury, $P = 0.3$), ruling out a large loss of cells by cell death, in agreement with previous studies^{1,2}. The number of single-labeled forelimb corticospinal neurons in the hindlimb field also remained unchanged (487 ± 72 in acutely injured animals, 420 ± 84 one week after injury, 384 ± 47 three weeks after injury, 456 ± 53 twelve weeks after injury). These

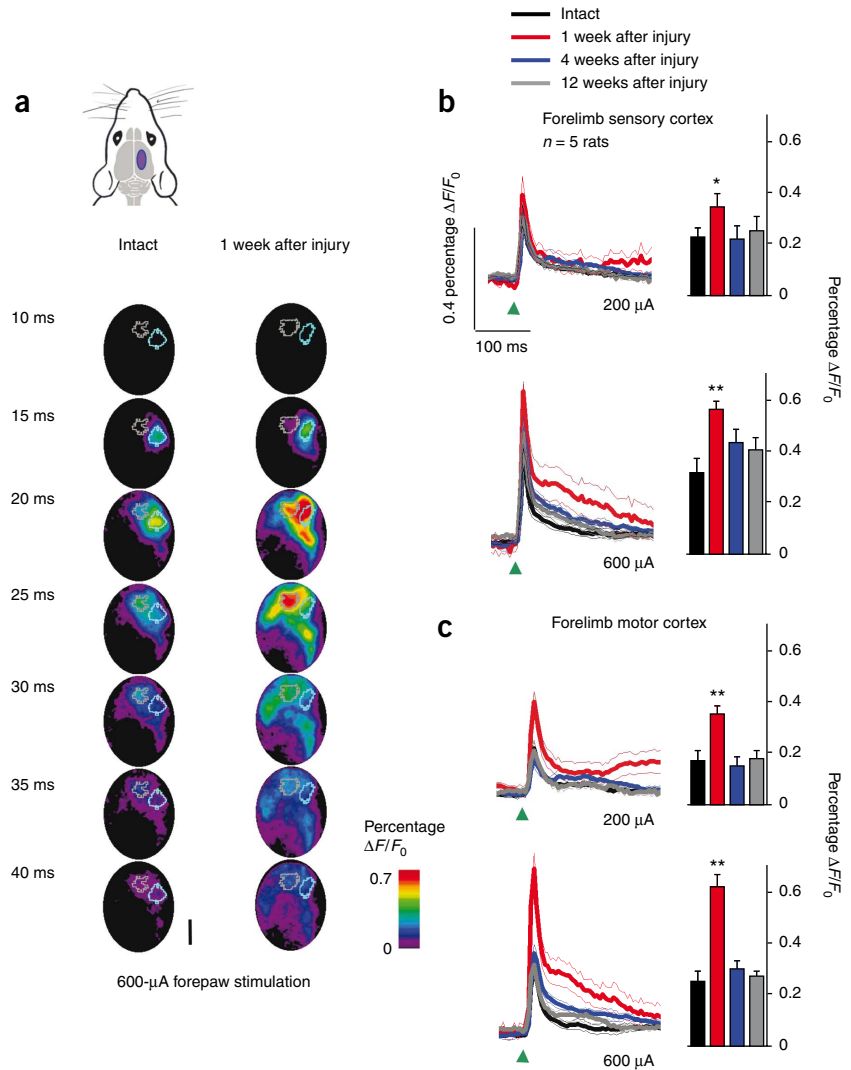
results show that axotomized hindlimb corticospinal neurons can increase their innervation of the cervical cord.

Representation of the forelimb as shown by BOLD-fMRI

The increase in fiber connections from axotomized hindlimb corticospinal neurons to the cervical spinal cord led us to ask whether forelimb sensory input can reach the hindlimb sensorimotor cortex. In the rat, forelimb sensory and motor cortices are well separated (as in higher mammals), but the hindlimb sensory and motor representations completely overlap²³. We mapped the activated regions after subcutaneous electrical stimulation of the forepaw and hindpaw (**Fig. 3**). We compared the effects of stimulation at 1.6 mA and 6 mA (3 Hz) to determine whether the detected map alterations depend on the stimulation current amplitude. The higher stimulation intensity has been used in BOLD-fMRI experiments under isoflurane anesthesia and is considered to be non-painful^{24,25}.

At the lower current stimulation, the forelimb representation of intact animals was confined to an area of 4.1 ± 0.3 mm² in the somatosensory cortex (**Fig. 3a,b,g**). We found no pre-existing overlap of forelimb and hindlimb somatosensory representations (**Fig. 3b,g**). At no point after injury could BOLD activation be elicited after hindlimb stimulation. One week after injury, the area activated by forelimb stimulation expanded to 7.0 ± 0.85 mm² ($P = 0.0135$, **Fig. 3c,d,g**). This expanded area included regions mostly medial to the original forelimb representation (**Fig. 3c,d**). Parts of the original hindlimb representation also responded to forelimb stimulation (**Fig. 3c,d,g**). This response was consistent across animals and occurred mainly in the rostral part of the hindlimb representation. Three weeks later the enlarged forelimb representation, overlapping with the rostral part of the original hindlimb field, remained (**Fig. 3e,f,g**). The non-invasive nature of BOLD-fMRI allowed us to follow up individual animals,

Figure 4 Voltage-sensitive dye imaging of the sensory and motor cortices responding to forelimb stimulation before and after injury. (a) Spatio-temporal dynamics of VSD signals in intact and injured rats, one week after injury. The diagram of the rat head shows the field of view (purple) used to detect responses after contralateral forepaw stimulation. Blue and gray outlines show 50% isocentric contours at 15 ms and 25 ms after stimulation, respectively. The 15 ms contour corresponds anatomically to and is used as the forelimb sensory region of interest. The 25 ms contour corresponds anatomically to and is used as the forelimb motor region of interest. (b,c) Mean time activation curves at different time points after injury with quantification of peak amplitude expressed as column plots. Regions of interest were the forelimb sensory cortex in **b** and the forelimb motor cortex in **c**. Stimulation intensity is mentioned below the activation curves. Thin lines and error bars represent \pm s.e.m. $n = 5$ rats, data were subjected to Mann-Whitney U test, * $P < 0.05$, ** $P < 0.01$. Green arrowhead points to the time of stimulation. Scale bar, 1.5 mm.



and we found that all animals had enlarged forelimb representations 1 week after injury (Supplementary Fig. 2). To what extent is the map expansion into the rostral portion of hindlimb field opportunistic? Although only a fraction of the expansion covered the hindlimb field, the area of overlap increased proportionally with the change in forelimb map size (Supplementary Fig. 2). Most of the expansion occurred medially into the forelimb motor area, suggesting that there was an increase in sensorimotor excitability in addition to an opportunistic encroachment of the hindlimb field after injury.

At the higher current stimulation, the area occupied by the forelimb representation in intact animals was in the same range as in the lower stimulation (3.8 ± 0.4 mm², Fig. 3g,h). Similarly, forelimb and hindlimb representations were well separated (Fig. 3h and Supplementary Fig. 3). One week after injury, the higher stimulation revealed an expansion into the rostral hindlimb field that remained for up to 12 weeks (Fig. 3h and see Supplementary Fig. 3). In addition, the forelimb maps were markedly larger when stimulated with the 6-mA current stimulation than the 1.6-mA current at 1 week after injury (12.4 ± 1.6 mm², Fig. 3g,h).

Voltage-sensitive dye imaging of the sensorimotor cortex

Next we addressed the spatio-temporal dynamics of forelimb sensory input in the sensorimotor cortex with a temporal resolution of 5 ms using VSD imaging. In comparison to BOLD-fMRI experiments, much lower stimulation strengths could be used under the same level of anesthesia, highlighting the sensitivity of VSD imaging: the forepaw was stimulated subcutaneously with a 1-ms pulse of current (200 or 600 μ A). In intact rats, neuronal responses in the forelimb sensory cortex were seen at a latency of 15 ms (Fig. 4a). In the following 5–10 ms, the activation spread medially to the forelimb motor cortex. One week after spinal cord injury, the same stimulation resulted in a stronger and larger response at the forelimb sensory cortex (Fig. 4a).

At 20–25 ms after stimulation, both forelimb sensory and motor cortices were highly activated compared to intact animals. In the following milliseconds the activation encompassed regions caudal to the original forelimb motor cortex, the hindlimb sensorimotor cortex as described later. To quantify the activations, two regions of interest were identified: the forelimb sensory cortex and the forelimb motor cortex. In response to the low (200 μ A) and high current (600 μ A) stimulations, both the sensory and motor cortices showed increased activation one week after injury (Fig. 4a–c); for example, at 600 μ A stimulation, the forelimb sensory cortex increased its activation from $0.32 \pm 0.05\%$ $\Delta F/F_0$ to $0.57 \pm 0.03\%$ $\Delta F/F_0$ ($P = 0.009$). The increased activations were absent 4 or 12 weeks after injury (Fig. 4b,c). In intact animals, the sensory cortex response amplitude of 0.3% $\Delta F/F_0$ (at 600 μ A) resulted in a slightly weaker activation of the motor cortex reflected by a motor:sensory cortex activation ratio of 0.8 ± 0.1 . One week after injury, at 200 μ A stimulation, the sensory response amplitude was 0.3% $\Delta F/F_0$, and the subsequent activation in the motor cortex was equally strong resulting in a ratio of 1.1 ± 0.1 . Therefore, the relative excitability of the motor cortex was higher after spinal cord injury ($P = 0.036$).

Next, we again investigated the activation of the hindlimb sensorimotor cortex by forelimb sensory input after injury. We estimated the hindlimb field using two approaches. The first relies on the localization

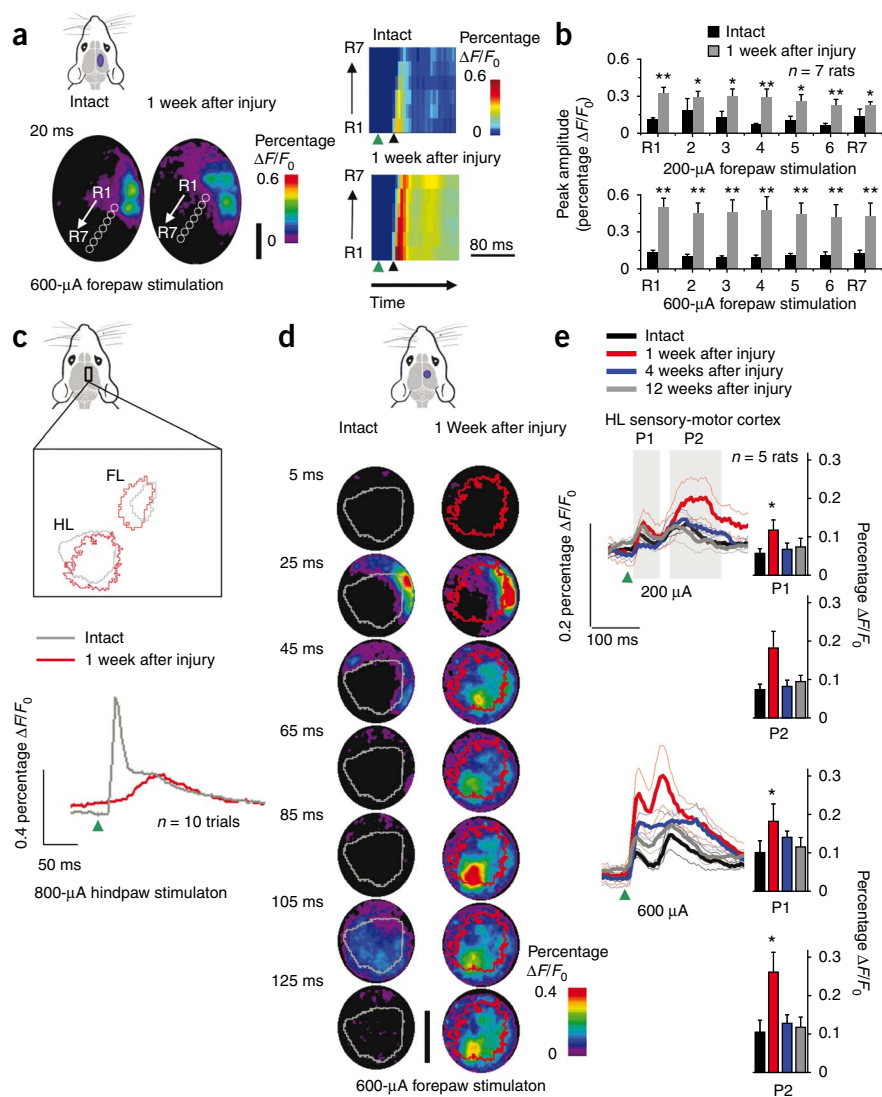


Figure 5 Response of the hindlimb sensorimotor cortex to forelimb stimulation in intact and injured rats. **(a)** Top left: a schematic view of the rat head showing the region of data acquisition in purple. The hindlimb field lies caudo-medial to the forelimb sensory cortex. Bottom left: seven 300- μ m diameter circular ROIs (R1–R7 white circles) were placed adjacent to the forelimb representation such that R1 included the caudal edge of the 50% isocentric contour drawn 20 ms after forepaw stimulation. The ROIs were placed at an angle of 35° from the midline. Right: activation representations in the ROIs. Note that the ROIs closest to the forelimb are activated first and the activation is much higher in all ROIs after injury. Green arrowheads in all panels point to the time of stimulation. Black arrowhead in **a** points to 20 ms after stimulation. **(b)** Quantification of activations in the distinct ROIs show strong activity in the hindlimb field after spinal cord injury at both 200 and 600 μ A stimulations. **(c)** Representative, superimposed, 50% isocentric contours at the time of peak response amplitude evoked by hindpaw stimulation (HL; 800 μ A current) in an intact (gray outline) and injured (red outline, one week after injury) rat and at 15 ms after forepaw stimulation (FL; 600 μ A current). Below, time activation curves of the enclosed hindlimb area responding to 800 μ A hindpaw stimulation. **(d)** Representative spatio-temporal dynamics of neuronal activity after forepaw stimulation in the identified hindlimb cortex in intact and injured rats. Grey and red outlines as in **c**. **(e)** Mean time activation curves of responses in the hindlimb cortex after forelimb stimulation and column plots of peak response amplitude in the two temporal blocks P1 and P2. Stimulation intensity is indicated below the plots. $n = 5$ rats, statistics are as described in **Figure 4**. Scale bars, 1.5 mm.

of the forelimb representation and its known spatial relationship to the hindlimb field, and the second is based on the activation of the hindlimb field in lesioned animals by stimulation of the spared spinothalamic tract. In intact animals the hindlimb area is caudo-medial to the forelimb sensorimotor field. We therefore assessed the hindlimb area in injured animals by placing seven adjacent regions of interest (ROIs) 35° from the midline starting with the caudal part of the forelimb field. In intact animals, forepaw stimulation resulted in low-amplitude activation of the hindlimb ROIs (**Fig. 5a,b**). The activation appeared first in the ROI closest to the forelimb area and last in the ROI farthest away. One week after injury, all the ROIs showed sequential activation at a much higher amplitude (**Fig. 5a,b**).

The second approach relied on activation of the spared spinothalamic tract. Inputs from this tract reach the hindlimb cortical areas that respond to tactile sensory input²⁶. Stimulation at 800 μ A resulted in a weak and delayed activation of the hindlimb area (**Fig. 5c**). In intact animals, the hindlimb sensorimotor area received forelimb sensory input 25 ms after stimulation in a very restricted rostro-lateral border area only. A second more general, weaker wave of activation occurred at ~100 ms (**Fig. 5d**). The first activation occurred exclusively at the rostral rim of the hindlimb sensorimotor area in proximity to the CFA. The second wave included the caudal aspects of the hindlimb

field. One week after injury, the initial activation at 25 ms was much stronger and encroached well into the hindlimb field (**Fig. 5d**). The second wave of activation occurred sooner, appearing by 45 ms and peaking at 85 ms in the caudal hindlimb field. We quantified the activations in the identified hindlimb area after 200 and 600 μ A forepaw stimulations (**Fig. 5e**). At the low current stimulation, the amplitude of the first wave of activation was significantly higher one week after injury. Both waves of activation had significantly higher amplitudes when the forepaw was stimulated at 600 μ A. Four and twelve weeks after injury, the rostral rim and the caudal hindlimb field continued to respond to forelimb stimulation (**Fig. 5e**). These results show that the hindlimb sensorimotor cortex in paraparetic rats responds to forelimb sensory input.

Response of hindlimb corticospinal axons to forelimb input

From both BOLD-fMRI and VSD imaging, we conclude that the denervated hindlimb sensorimotor area receives forelimb sensory input. However, it remains unclear whether this sensory input activates hindlimb corticospinal neurons that originate from cortical layer V (which is too deep to be assessed by VSD imaging). Sensory input can induce action potentials in corticospinal neurons^{27–29}. It remains unknown whether forelimb sensory input reaches the hindlimb CST.

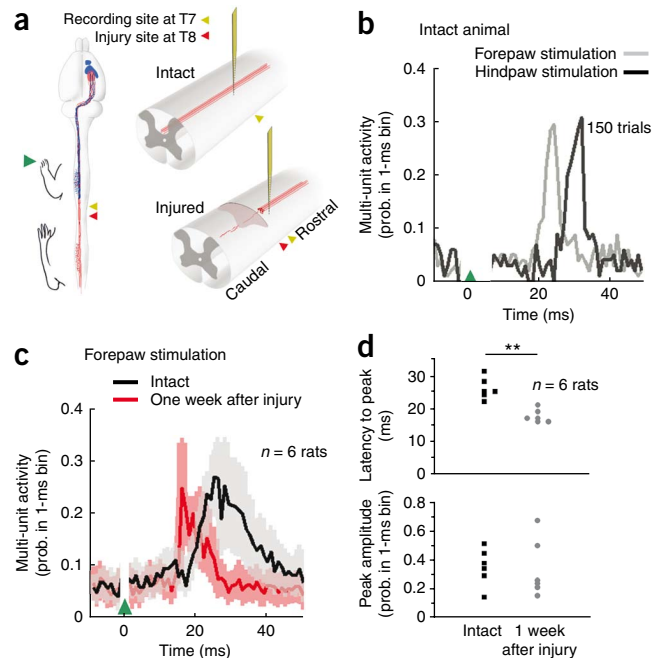
Figure 6 Forelimb stimulation evoked action potentials in the corticospinal tract at thoracic level T7. **(a)** The forelimb was stimulated at 6 mA (green arrowhead) for 1 ms and a probe with 16 electrodes inserted at T7 (golden arrowhead) was used to detect action potentials. Red arrowhead shows T8, the location of injury. **(b)** Peri-stimulus time histogram (PSTH, time block = 1 ms) of an intact rat responding to hindlimb and forelimb stimulation (6 mA, 1 ms). **(c)** Mean activation curves based on PSTH after forelimb stimulation in intact and injured animals ($n = 6$). Shaded area depicts \pm s.e.m. **(d)** Quantification of the latency to peak and peak amplitude from PSTH of intact and injured rats. $n = 6$ rats, statistics are as described in **Figure 4**. Green arrowhead points to the time of stimulation.

We recorded extracellular action potentials evoked by subcutaneous forepaw stimulation from the CST at level T7 (multi-unit extracellular recordings) in intact and injured animals. Most of these axons project to the lumbar enlargement and are therefore involved in hindlimb function. Recording from the hindlimb CST in the spinal cord we could specifically address the changes in this cell type after injury. First, we stimulated the hindlimb of four intact rats to determine that at 6 mA current stimulation (1 pulse, 1 ms) the CST response was significant (**Fig. 6a,b**). In intact animals, forelimb stimulation resulted in a significant response in T7 CST axons at 22–32 ms (latency to peak amplitude, mean 27 ± 2 ms, $n = 4$) after stimulation, 6 ms faster than the response to hindlimb stimulation (mean 33 ± 1 ms, $n = 4$). One week after injury at T8, the hindlimb CST responses to the forelimb stimulation were markedly faster, with a latency to peak at 18 ± 1 ms ($n = 6$, **Fig. 6c,d**). In both groups, the number of spikes detected varied greatly between animals, probably due to a lack of distinction between single and compound action potentials and differences in the positioning of the $177 \mu\text{m}^2$ electrode in the densely packed CST (**Fig. 6d**). Importantly, there was no correlation between the latency to peak amplitude and the amplitude itself in the injured group. However, intact animals showed a tendency for longer latency to peak with increase in amplitude of the response ($r^2 = 0.55$, linear fit, **Supplementary Fig. 4**). The responses in the CST of both intact and injured animals could be eliminated by cortical ablation that included the hindlimb area (**Supplementary Fig. 5**). Therefore, axotomized hindlimb corticospinal neurons can respond to sensory input from the forelimb. This input might contribute to the rewiring and forelimb function of the hindlimb neurons after spinal cord injury.

DISCUSSION

We have shown that, in response to a thoracic bilateral dorsal hemisection, which renders the hindlimbs dysfunctional, about 10% of the axotomized hindlimb corticospinal neurons rewired to the cervical spinal cord. Over months, about 50% of these rewired neurons were eliminated from the cervical segments but neurons in the rostral hindlimb domain, in proximity to the forelimb cortex, remained. Using VSD imaging and BOLD-fMRI of the cortex, we showed that the forelimb sensory representation was altered after injury and expanded into the hindlimb sensorimotor area. The enhanced forelimb sensory input into the hindlimb sensorimotor cortex was also reflected at the level of the hindlimb corticospinal neurons responding to forelimb sensory input (see **Supplementary Fig. 6** for a schematic summary).

After a thoracic injury, the hindlimbs showed no spontaneous recovery in the skilled walking tasks. Owing to the significant steps taken in the last decade to induce regeneration in the adult CNS, it is now envisioned that spinal cord injury treatments that promote regeneration and structural plasticity will eventually lead to functional improvements⁴. However, our understanding of the changes induced by the injury itself remains incomplete. Do axotomized



corticospinal cells remain dormant after injury? Our data show that the cells can form new connections, distant from the site of injury. The presented number of rewired corticospinal neurons (detected as double-labeled neurons) is a gross underestimate, when the efficiencies of tracers used are taken into account. Retrograde labeling from the site of injury at T8 with the dextran dye Mini-ruby labeled ~4,900 corticospinal neurons. We estimate that the labeling reveals only about one-seventh of the corticospinal axons that pass through the thoracic spinal cord, according to axonal counts³⁰. The other tracer, Fast Blue, labels ~1.5 times more cells than the dextran³¹. Therefore, we expect that the number of rewired corticospinal neurons is at least seven times higher than is shown by the retrograde method.

Adult neurons in the CNS cannot regenerate over long distances, but axotomized neurons can form short sprouts from their damaged axons^{32–34}. Previously, anterograde tracing experiments in the adult rat after thoracic injury showed that corticospinal neurons from the hindlimb cortex can sprout into the cervical spinal cord gray matter^{7,8}. Here, retrograde tracing allowed us to identify axotomized hindlimb neurons that rewired to cervical segments. This rewiring might involve the formation of entirely new axonal collaterals and/or the enlargement of rare pre-existing axonal arbors in the cervical gray matter after axotomy; very few collaterals of the hindlimb axons into the cervical spinal cord were detected in intact animals by using anterograde tracing, confirming the present retrograde tracing results. Counts and topographic maps of the rewired neurons showed that some pruning followed within several weeks after the initial sprouting of the axotomized hindlimb axons in the cervical segments. In agreement with the anterograde experiments, about half of the rewired hindlimb neurons remained connected to the cervical spinal cord^{7,8}. Neurons that did not undergo pruning were mostly located in the rostral part of the hindlimb field, in proximity to the original forelimb corticospinal area. The forelimb corticospinal representation is thus permanently strengthened by recruitment of former hindlimb CST neurons. These rewired axons presumably connect to the spinal neurons in cervical cord and the significance of this is demonstrated by the existence of forelimb movements upon intracortical stimulation of the hindlimb cortex after thoracic spinal cord injury⁸. The persistence of rewired

neurons in proximity to the forelimb cortex could suggest a role for forelimb inputs in inducing sprouting or determining the fate of the axotomized sprouting corticospinal neurons.

After focal forelimb cortical stroke, hindlimb neurons (in the superficial layers) become responsive to forelimb sensory input³⁵. After a spinal cord injury, if the anatomically rewired hindlimb sensorimotor cortex is to participate in meaningful forelimb movements, it must also receive forelimb sensory input and be responsive to it. To address this, we used VSD imaging and BOLD-fMRI. Studies in paraplegic humans failed to agree whether the denervated leg representation in the sensory cortex becomes responsive to input from the hand^{36,37}. In paraplegic rats too, an expansion of the forelimb sensory representation into neighboring cortical areas including the hindlimb sensorimotor cortex has been described using BOLD-fMRI, but an electrophysiological study failed to observe such an activation^{13,14}. In our study, using forepaw electrical stimulation, BOLD-fMRI of intact animals revealed exclusive activation of the forelimb sensory cortex. In contrast, VSD imaging revealed a robust additional activation of the forelimb motor cortex (medial to forelimb sensory cortex). After injury, the BOLD response area expanded medially to the forelimb motor cortex. This shows that pre-existing forelimb sensorimotor circuits change significantly after injury to result in an expanded BOLD activation area. The rewired CST representation continues to refine over weeks after injury. Based on the BOLD results it would be premature for us to conclude that refinement of the sensory input does not take place. A better understanding of the relationship between anatomical rewiring and BOLD map alterations would be possible if these measurements were taken from the same animal. Importantly, the rostral part of the hindlimb representation, in both BOLD-fMRI and VSD experiments, responded consistently to forelimb sensory stimulation after injury. Thus, the denervated hindlimb sensorimotor cortex receives forelimb sensory inputs after spinal cord lesion. The expansion of the forelimb representation into the hindlimb field and the alteration of the forelimb sensorimotor circuitry might be related to the increased behavioral reliance of the rats on their forelimbs after injury.

Using extracellular recordings, we found that axotomized hindlimb corticospinal neurons responded faster to sensory inputs from the forelimb than when intact. Exactly which aspect of the sensory input these cells were responding to remains unclear given the strength of the stimulus used. Both the sensory current threshold for CST activation and the pathways involved remain unidentified. Moreover, given that our recordings rostral to the injury might include axotomized axons that do and that do not give rise to collaterals in the cervical spinal cord, it remains unclear whether the rewired neurons respond faster to inputs from the forelimb. Shorter latency to cortical responses from injury spared body parts has been previously observed in experiments involving digit denervation, within hours of injury³⁸. In agreement with a previous *in vitro* study, we find that axotomized corticospinal neurons not only survive the injury but also continue to respond to synaptic input³⁹. Our VSD imaging experiments show that the forelimb sensory cortex, the forelimb motor cortex and the hindlimb sensorimotor cortex are all more excitable in response to forelimb sensory input after injury. With two different amplitudes of stimulation, resulting in the same response amplitude in the sensory cortex before and after injury, we showed that the forelimb motor cortex is more excitable one week after injury. Changes in cellular physiology, synaptic strength and intra- and sub-cortical circuits might all contribute to the faster response of the axotomized hindlimb CST in paraparetic rats.

The observed excitability in the forelimb sensorimotor cortex within 7 days of spinal cord injury might in particular be due to

altered effectiveness of horizontal connections⁴⁰. The suppression of GABA-mediated inhibition might unmask pre-existing horizontal connections, leading to enlarged cortical activation maps⁴¹. With reduced intra-cortical inhibition, synaptic strengthening of excitatory horizontal inputs to pyramidal neurons is likely⁴². The suggested alterations to the input of axotomized corticospinal neurons might also lead to changes in the cortical 'hardware', including axonal arbors and dendrites. Notably, in adult mice after a spinal cord injury, there is an initial loss of dendritic spine density in layer V pyramidal neurons in the motor cortex⁴³. This loss is partially reversed within a few weeks after injury. It remains to be determined whether the changes reported in our study are driven by the behavioral compensations by the forelimb. It is known that learning of a new motor skill results in increased excitability of the motor cortex⁴⁴. Therefore, we speculate that the increased forelimb use results in alterations in cortical excitability that then influences anatomical alterations of the axotomized corticospinal neurons. This speculation is in line with earlier studies that show that cortical activity can influence sprouting of the CST⁴⁵.

In summary, we observed significant alterations in how the sensorimotor cortex received and processed inputs from the forelimb after a thoracic spinal cord injury. The forelimb sensory representation expanded and invaded parts of the denervated hindlimb area. The regions in the hindlimb cortex that received forelimb sensory input gave rise to collaterals in the cervical spinal cord from axotomized neurons. Thus, axotomized corticospinal neurons re-wire after injury and are incorporated into the circuitry of the injury-spared body part.

METHODS

Methods and any associated references are available in the online version of the paper at <http://www.nature.com/natureneuroscience/>.

Note: Supplementary information is available on the Nature Neuroscience website.

ACKNOWLEDGMENTS

We thank J. Scholl, E. Hochreutener, R. Schöb and L. Schnell for technical assistance. We thank A. Buchli, I. Maier, M. Starkey, V. Pernet, D. Margolis and B. Kampa for helpful discussions. This work was supported by the Swiss National Science Foundation, Grant 31-63633.00, the National Center of Competence in Research "Neural Plasticity and Repair" of the Swiss National Science Foundation, the Spinal Cord Consortium of the Christopher Reeve Paralysis Foundation, and NeuroNe, Network of Excellence of the European Consortium for Research in Neurodegenerative Diseases (Sixth Framework EU Program).

AUTHOR CONTRIBUTIONS

A.G. and M.E.S. designed the experiments and prepared the manuscript. A.G., F.H. and E.S. carried out and interpreted the experiments. R.S., M.G., M.T.W., T.M. and C.B. performed the experiments. M.R. and B.W. prepared the manuscript.

Published online at <http://www.nature.com/natureneuroscience/>.

Reprints and permissions information is available online at <http://www.nature.com/reprintsandpermissions/>.

1. Kalil, K. & Schneider, G.E. Retrograde cortical and axonal changes following lesions of the pyramidal tract. *Brain Res.* **89**, 15–27 (1975).
2. Wannier, T., Schmidlin, E., Bloch, J. & Rouiller, E.M. A unilateral section of the corticospinal tract at cervical level in primate does not lead to measurable cell loss in motor cortex. *J. Neurotrauma* **22**, 703–717 (2005).
3. Hains, B.C., Black, J.A. & Waxman, S.G. Primary cortical motor neurons undergo apoptosis after axotomizing spinal cord injury. *J. Comp. Neurol.* **462**, 328–341 (2003).
4. Maier, I.C. & Schwab, M.E. Sprouting, regeneration and circuit formation in the injured spinal cord: factors and activity. *Phil. Trans. R. Soc. Lond. B* **361**, 1611–1634 (2006).
5. Raineteau, O. & Schwab, M.E. Plasticity of motor systems after incomplete spinal cord injury. *Nat. Rev. Neurosci.* **2**, 263–273 (2001).
6. Aoki, M., Fujito, Y., Satomi, H., Kurosawa, Y. & Kasaba, T. The possible role of collateral sprouting in the functional restitution of corticospinal connections after spinal hemisection. *Neurosci. Res.* **3**, 617–627 (1986).

7. Bareyre, F.M. *et al.* The injured spinal cord spontaneously forms a new intraspinal circuit in adult rats. *Nat. Neurosci.* **7**, 269–277 (2004).
8. Fouad, K., Pedersen, V., Schwab, M.E. & Brosamle, C. Cervical sprouting of corticospinal fibers after thoracic spinal cord injury accompanies shifts in evoked motor responses. *Curr. Biol.* **11**, 1766–1770 (2001).
9. Weidner, N., Ner, A., Salimi, N. & Tuszynski, M.H. Spontaneous corticospinal axonal plasticity and functional recovery after adult central nervous system injury. *Proc. Natl. Acad. Sci. USA* **98**, 3513–3518 (2001).
10. Ghosh, A. *et al.* Functional and anatomical reorganization of the sensory-motor cortex after incomplete spinal cord injury in adult rats. *J. Neurosci.* **29**, 12210–12219 (2009).
11. Kaas, J.H. *et al.* Cortical and subcortical plasticity in the brains of humans, primates, and rats after damage to sensory afferents in the dorsal columns of the spinal cord. *Exp. Neurol.* **209**, 407–416 (2008).
12. Jain, N., Florence, S.L., Qi, H.X. & Kaas, J.H. Growth of new brainstem connections in adult monkeys with massive sensory loss. *Proc. Natl. Acad. Sci. USA* **97**, 5546–5550 (2000).
13. Endo, T., Spenger, C., Tominaga, T., Brene, S. & Olson, L. Cortical sensory map rearrangement after spinal cord injury: fMRI responses linked to Nogo signalling. *Brain* **130**, 2951–2961 (2007).
14. Jain, N., Florence, S.L. & Kaas, J.H. Limits on plasticity in somatosensory cortex of adult rats: hindlimb cortex is not reactivated after dorsal column section. *J. Neurophysiol.* **73**, 1537–1546 (1995).
15. Wall, P.D. & Egger, M.D. Formation of new connexions in adult rat brains after partial deafferentation. *Nature* **232**, 542–545 (1971).
16. Liebscher, T. *et al.* Nogo-A antibody improves regeneration and locomotion of spinal cord-injured rats. *Ann. Neurol.* **58**, 706–719 (2005).
17. Schucht, P., Raineteau, O., Schwab, M.E. & Fouad, K. Anatomical correlates of locomotor recovery following dorsal and ventral lesions of the rat spinal cord. *Exp. Neurol.* **176**, 143–153 (2002).
18. Hamers, F.P., Koopmans, G.C. & Joosten, E.A. CatWalk-assisted gait analysis in the assessment of spinal cord injury. *J. Neurotrauma* **23**, 537–548 (2006).
19. Metz, G.A. & Whishaw, I.Q. Cortical and subcortical lesions impair skilled walking in the ladder rung walking test: a new task to evaluate fore- and hindlimb stepping, placing, and co-ordination. *J. Neurosci. Methods* **115**, 169–179 (2002).
20. Sievert, C.F. & Neafsey, E.J. A chronic unit study of the sensory properties of neurons in the forelimb areas of rat sensorimotor cortex. *Brain Res.* **381**, 15–23 (1986).
21. Neafsey, E.J. & Sievert, C. A second forelimb motor area exists in rat frontal cortex. *Brain Res.* **232**, 151–156 (1982).
22. Akintunde, A. & Buxton, D.F. Differential sites of origin and collateralization of corticospinal neurons in the rat: a multiple fluorescent retrograde tracer study. *Brain Res.* **575**, 86–92 (1992).
23. Hall, R.D. & Lindholm, E.P. Organization of motor and somatosensory neocortex in the albino rat. *Brain Res.* **66**, 23–38 (1974).
24. Liu, Z.M., Schmidt, K.F., Sicard, K.M. & Duong, T.Q. Imaging oxygen consumption in forepaw somatosensory stimulation in rats under isoflurane anesthesia. *Magn. Reson. Med.* **52**, 277–285 (2004).
25. Sicard, K.M. & Duong, T.Q. Effects of hypoxia, hyperoxia, and hypercapnia on baseline and stimulus-evoked BOLD, CBF, and CMRO₂ in spontaneously breathing animals. *Neuroimage* **25**, 850–858 (2005).
26. Guilbaud, G., Benoist, J.M., Levante, A., Gautron, M. & Willer, J.C. Primary somatosensory cortex in rats with pain-related behaviors due to a peripheral mononeuropathy after moderate ligation of one sciatic nerve: neuronal responsiveness to somatic stimulation. *Exp. Brain Res.* **92**, 227–245 (1992).
27. Adrian, E.D. & Moruzzi, G. Impulses in the pyramidal tract. *J. Physiol. (Lond.)* **97**, 153–199 (1939).
28. Swett, J.E. & Bourassa, C.M. Short latency activation of pyramidal tract cells by Group I afferent volleys in the cat. *J. Physiol. (Lond.)* **189**, 101–117 (1967).
29. McComas, A.J. & Wilson, P. An investigation of pyramidal tract cells in the somatosensory cortex of the rat. *J. Physiol. (Lond.)* **194**, 271–288 (1968).
30. Schreyer, D.J. & Jones, E.G. Axon elimination in the developing corticospinal tract of the rat. *Brain Res.* **466**, 103–119 (1988).
31. Choi, D., Li, D. & Raisman, G. Fluorescent retrograde neuronal tracers that label the rat facial nucleus: a comparison of Fast Blue, Fluoro-ruby, Fluoro-emerald, Fluoro-Gold and Dil. *J. Neurosci. Methods* **117**, 167–172 (2002).
32. Schwab, M.E. & Bartholdi, D. Degeneration and regeneration of axons in the lesioned spinal cord. *Physiol. Rev.* **76**, 319–370 (1996).
33. Fawcett, J.W. & Geller, H.M. Regeneration in the CNS: optimism mounts. *Trends Neurosci.* **21**, 179–180 (1998).
34. Foerster, A.P. Spontaneous regeneration of cut axons in adult rat brain. *J. Comp. Neurol.* **210**, 335–356 (1982).
35. Brown, C.E., Aminoltejeri, K., Erb, H., Winship, I.R. & Murphy, T.H. *In vivo* voltage-sensitive dye imaging in adult mice reveals that somatosensory maps lost to stroke are replaced over weeks by new structural and functional circuits with prolonged modes of activation within both the peri-infarct zone and distant sites. *J. Neurosci.* **29**, 1719–1734 (2009).
36. Turner, J.A., Lee, J.S., Schandler, S.L. & Cohen, M.J. An fMRI investigation of hand representation in paraplegic humans. *Neurorehabil. Neural Repair* **17**, 37–47 (2003).
37. Curt, A., Bruehlmeier, M., Leenders, K.L., Roelcke, U. & Dietz, V. Differential effect of spinal cord injury and functional impairment on human brain activation. *J. Neurotrauma* **19**, 43–51 (2002).
38. Doetsch, G.S., Harrison, T.A., MacDonald, A.C. & Litaker, M.S. Short-term plasticity in primary somatosensory cortex of the rat: rapid changes in magnitudes and latencies of neuronal responses following digit denervation. *Exp. Brain Res.* **112**, 505–512 (1996).
39. Tseng, G.F. & Prince, D.A. Structural and functional alterations in rat corticospinal neurons after axotomy. *J. Neurophysiol.* **75**, 248–267 (1996).
40. Huntley, G.W. Correlation between patterns of horizontal connectivity and the extend of short-term representational plasticity in rat motor cortex. *Cereb. Cortex* **7**, 143–156 (1997).
41. Jacobs, K.M. & Donoghue, J.P. Reshaping the cortical motor map by unmasking latent intracortical connections. *Science* **251**, 944–947 (1991).
42. Hess, G. & Donoghue, J.P. Long-term potentiation of horizontal connections provides a mechanism to reorganize cortical motor maps. *J. Neurophysiol.* **71**, 2543–2547 (1994).
43. Kim, B.G., Dai, H.N., McAtee, M., Vicini, S. & Bregman, B.S. Remodeling of synaptic structures in the motor cortex following spinal cord injury. *Exp. Neurol.* **198**, 401–415 (2006).
44. Rosenkranz, K., Williamon, A. & Rothwell, J.C. Motorcortical excitability and synaptic plasticity is enhanced in professional musicians. *J. Neurosci.* **27**, 5200–5206 (2007).
45. Salimi, I., Friel, K.M. & Martin, J.H. Pyramidal tract stimulation restores normal corticospinal tract connections and visuomotor skill after early postnatal motor cortex activity blockade. *J. Neurosci.* **28**, 7426–7434 (2008).

ONLINE METHODS

Experimental subjects. Adult female Lewis rats (200–220 g, obtained from R. Janvier, Le Genest-St Isle, France) were used. Animals were housed in groups of four in standardized cages (Marcolon type IV) at a 12:12 h light:dark cycle with food and water *ad libitum*. All animals were given one week to acclimatize to their housing before experimentation. All experimental procedures performed were in adherence to the guidelines of the Veterinary office of the Canton of Zurich, Switzerland.

Spinal cord injury. Spinal cord dorsal bilateral hemisections were performed as described elsewhere⁷. Briefly, a dorsal bilateral laminectomy was performed at thoracic segment 8 (vertebra) under anesthesia (Hypnorm, 120 μ l per 200 g body weight subcutaneous (VetaPharma) and Dormicum, 0.75 mg in 150 μ l per 200 g body weight subcutaneous (Roche Pharmaceuticals)). Using sharp iridectomy scissors, the dorsal half of the spinal cord was transected (**Supplementary Fig. 1**). The retrograde tracer was applied to the injury site as described below. After surgery, animals were administered analgesic (2.5 mg per kg of body weight subcutaneous injection of Rimadyl; Pfizer Laboratories) once a day for five days and antibiotic (Baytril 1.25 mg per 250 g body weight intraperitoneal; Bayer AG) once a day for five days. Bladders were checked and emptied three times a day until bladder function had completely recovered. Spinal cord injuries were histologically verified. Inadequately injured or over-lesioned rats were subsequently eliminated from analysis.

Behavioral data acquisition and analysis. Animals were evaluated on the Catwalk^R (Noldus Information Technology) and on the horizontal ladder. Before injury, animals were trained on the behavioral tests for 3 weeks (twice per week in the first 2 weeks, once in the following week). The catwalk analysis system has been described in detail¹⁸. Briefly, this system consists of a glass runway, with customized lighting, which is video recorded as the animals traverse the runway. From these videos the system determines the percentage of usage by each paw and the intensity of footprints during maximum paw contact at every step.

The horizontal ladder consists of equally spaced (at 6-cm gaps) rungs. The ladder was 1 m long and elevated at 1 m. Three trials were video recorded over a 60-cm stretch. Videos were analyzed offline. When the paw was placed such that the limb did not slip from the rung (weight-supported steps), a step was noted as successful¹⁰. The percentage of correct placements for each animal was determined by averaging over three trials.

Retrograde tracing and labeled cell analysis. After a spinal cord injury was performed as described above, 2 μ l of retrograde tracer Mini Ruby (a 3,000 MW dextran conjugated to tetra-methyl rhodamine, 10% in 0.1M PB; Invitrogen) was placed at the site of injury. Twenty minutes later, excess dye seeping out of the lesion site was removed by placing a sterile cotton piece on the dorsal surface of the injured cord, covering the lesion for 10–15 min. Injections into the cervical gray matter were done using a modified stereotaxic frame under deep anesthesia (Hypnorm and Dormicum as mentioned above); the head was fixed using ear bars and the cervical vertebra was fixed using clamps placed on either side of the vertebral column. A unilateral laminectomy was performed at C6 and C7 and the dura was removed. Using a 28 G Nanofil syringe attached to an UltraMicroPump (WPI) mounted on the stereotaxic frame, 1% Fast Blue (EMS-Polyloy) suspension in 0.1 M PB and 2% DMSO was injected into the spinal cord. The injection was monitored with fluorescence binoculars. Each animal had five injections of 120 nl of Fast Blue spaced at 0.5 mm, along the spinal cord. The coordinates for injection were 0.75 mm lateral from the midline and 1.2 mm below the spinal cord surface. Unilaterality of the injection was verified post-mortem. Ten days after injections, animals were perfused with paraformaldehyde (4%, post-fixed for 4 h after perfusion) and processed for cryosectioning in 30% sucrose. Series of 50- μ m spinal cord sections of the injection site in the cervical segment confirmed the confinement of the tracer to the cervical gray matter and lack of spread into the densely packed white matter. Series of 50- μ m brain cross-sections (with 100- μ m gaps) were used for quantification of labeled cells (cell counts were multiplied by 3 to incorporate the skipped sections into our estimate of the number of cells per hemisphere) and for the reconstruction of forelimb and hindlimb corticospinal representations. Fast Blue, Mini Ruby and double-labeled neurons were identified on a fluorescent microscope configured

to Neurolucida (ver 7.0; MicroBrightfield). Apparent double-labeled cells with a faint label of either tracer were confirmed using confocal microscopy.

BOLD fMRI. Rats were scanned before and after spinal cord injury on a Bruker Biospec 94/30 horizontal bore small animal MR system (BGA-12 gradient insert; gradient strength 400 mT m⁻¹, minimum rise time of 80 μ s; Bruker Biospin GmbH) under isoflurane anesthesia (1.5%). The muscle relaxant Gallamine (3 mg per 200 g bodyweight; Sigma-Aldrich) was used to immobilize the animals. Anatomical images were obtained using a multi-slice rapid acquisition with relaxation enhancement (RARE) spin echo sequence (parameters: field of view (FOV) = 53 \times 25 mm², matrix dimension (MD) = 256 \times 128, slice thickness (SLTH) = 1 mm, inter-slice distance (ISD) = 1.25 mm, echo delay (TE) = 60 ms, repetition delay (TR) = 1,259 ms, RARE factor = 8, number of acquisitions (NA) = 1, acquisition time T_{acq} = 1.25 min). BOLD-fMRI was performed using a serial gradient-echo echo-planar-imaging (GE-EPI) sequence (FOV = 33 \times 25 mm², MD = 64 \times 64, SLTH = 1 mm, temporal resolution = 10 s, 50 repetitions, T_{acq} = 8 min 20 s). Two horizontal images were acquired to cover all cortical layers. Both forepaws and the hindpaw were stimulated using needle electrodes placed subcutaneously. Stimulation parameters were: amplitude = 1.6–6 mA, pulse duration = 0.5 ms and frequency = 3 Hz. A repetitive block design has been used with 5 cycles consisting of an on-period of 40 s and an off-period of 60 s. Digit flexion threshold was determined before the application of Gallamine.

Data were analyzed using Biomap (ver. 4; Martin Rausch, Novartis) with statistical analysis done using a general linear model. Thresholds for considering activation were $P < 0.01$ and a minimum area of 3 voxels. Without further processing, these data were spatially normalized using landmarks identified directly on EPI images as described⁴⁶ (using custom-written software based on IDL (ITT)). Briefly, maximum intensity projections of the two horizontal sections were calculated and subsequently summed to generate overlapping maps (using a custom-written program based on Matlab (The MathWorks), extraction with t -value threshold of 4).

Optical imaging of the cortex using a voltage-sensitive dye. Optical imaging using the VSD RH1691 was performed as described, under isoflurane anesthesia (4% for induction, maintained at 1.5% during imaging, 3% while not imaging)^{10,47}. Briefly, the sensorimotor cortex was exposed carefully and the VSD (1 mg ml⁻¹ in Ringer's solution) was topically added and then allowed to diffuse for 1 h. The undiffused dye was washed from the surface using Ringer's solution. The cortex was then covered with 2% agar solution and with a glass coverslip. Animals were stimulated (subcutaneous forepaw or hindpaw electrodes) with a single pulse current (200–800 μ A amplitude, 1 ms duration). Stimulation strength as high as used in BOLD-fMRI resulted in saturation of the VSD signal and made the sensorimotor activation difficult to characterize. VSD was excited with 630 nm light from a 100-W halogen lamp. Images (100 \times 100 pixels, 6 \times 6 mm FOV, 5 ms exposure time) were acquired using a high speed CMOS camera (Micam Ultima, Scimedia). Analyses were based on a bleach-corrected average of 10 trials. Bleach correction (double exponential fit), conversion to changes in VSD fluorescence intensity (% $\Delta F/F_0$) and region-of-interest analysis were performed using PMOD (PMOD Technologies Ltd).

Multi-unit recordings from the CST. Animals under deep isoflurane anesthesia (ventilated, monitoring arterial pressure) were fixed on the modified stereotaxic frame as mentioned above, with the clamps placed on the thoracic vertebra. A laminectomy was performed at T7. A 16-channel NeuroNexus probe (16 probes spaced at 100 μ m, 0.7–1.4 M, NeuroNexus Technologies) coated with DiI was used to record multi-unit responses and descended into the dorsal funiculus 0.15 mm away from the midline. Prior to recording, isoflurane anesthesia was gradually replaced with Urethane (1,200 mg kg⁻¹ intraperitoneal, Sigma-Aldrich) and the muscle relaxant pancuronium bromide injected intravenous (0.1 mg kg⁻¹, Pavulon, Organon). Upon forepaw stimulation in injured animals and fore- or hindpaw stimulation in intact animals at 6 mA (1 ms), action potentials were initiated. The stimulation amplitude was based on a previous study²⁹. Responses from the corticospinal tract were obtained from electrodes at a depth of 1.0–1.2 mm. Before ablation, the cortex was stimulated using a platinum tungsten glass coated electrode (below 1 M Ω) placed in layer V of the hindlimb cortex or using a silver ball electrode (0.5 mm diameter) placed on the

surface of the hindlimb cortex to verify the CST response in a given channel. The hindlimb cortex was ablated using a suction device. See **Supplementary Note** and **Supplementary Fig. 5** for more detailed discussion and description of this method.

Statistics. Behavioral data were analyzed using an unpaired *t*-test. Anatomical and physiological data were analyzed using the Mann-Whitney U ranking test. In multi-unit recording experiments, 99% confidence limits (in **Supplementary**

Fig. 5) were estimated based on the assumption that the spike train is a Poisson train. Data are shown and stated as mean \pm s.e.m.

46. Sydekum, E. *et al.* Functional reorganization in rat somatosensory cortex assessed by fMRI: elastic image registration based on structural landmarks in fMRI images and application to spinal cord injured rats. *Neuroimage* **44**, 1345–1354 (2009).
47. Ferezou, I. *et al.* Spatiotemporal dynamics of cortical sensorimotor integration in behaving mice. *Neuron* **56**, 907–923 (2007).